Large Schottky-type heat capacity anomalies in liquid alkali group IV alloys

1995 J. Phys.: Condens. Matter 7 4803

(http://iopscience.iop.org/0953-8984/7/25/006)

J. Phys.: Condens. Matter 7 (1995) 4803–4820. Printed in the UK

Large Schottky-type heat capacity anomalies in liquid alkali group IV alloys

Wiebe Geertsma† and Marie-Louise Saboungi‡

† Solid State Physics Laboratory, 9747 AG Nijenborgh 4, Groningen, The Netherlands
‡ Argonne National Laboratory, 9700 South Cass Avenue, Argonne, IL 60439, USA

Received 22 March 1995

Abstract. The heat capacities of some liquid alkali–lead and alkali–tin alloys exhibit anomalous behaviour as a function of both composition and temperature. The equiatomic composition is characterized by a large excess heat capacity which depends strongly upon temperature. Taking into account the thermodynamic properties and structural measurements, we propose a model for these alloys based on a dissociation scheme of polyvalently charged anions into either free atoms, ions or some other small entities.

1. Introduction

A large number of experimental as well as theoretical investigations have been reported on the electronic and atomic structure of liquid alkali group IV alloy systems: van der Lugt and Geertsma (1987), Saboungi *et al* (1990a), van der Lugt (1991). The various experimental data like resistivities, Knight shifts, thermopowers, thermodynamics and structure on these alloys can be explained assuming the existence of rather long-living polyanions—so-called Zintl ions—in the liquid state. In this paper we present further evidence for this interpretation with a special emphasis on the thermodynamic results.

The heat capacity of the equiatomic alkali Pb compounds (Saboungi *et al* 1988, 1990a, b) takes dramatically large values just above the melting points, in the range of 60 to 70 J mol^{-1} K^{-1}, and decreases with temperature. The presence in the liquid of structural units, dissociating gradually with temperature, could explain qualitatively and quantitatively such a behaviour. Zintl ions were known to form in the corresponding solid intermetallic compounds and, based on the structural measurements, it was suggested that these survive the solid–liquid transition. The stability of these ions, schematically represented by M_4^{4-}, where M = Pb are located on a regular tetrahedron surrounded by an oppositely oriented and positively charged alkali metal tetrahedron, was shown to depend not only on the temperature of the liquid, but also on the nature of the cation.

Saar and Ruppersberg (1987, 1988) observed a similar behaviour of the heat capacity in the liquid alloy system Li_cPb_{1-c} which exhibits a strong peak of about 26 J mol^{-1} K^{-1} close to $c = 0.8$. Near this composition the excess heat capacity first decreases on heating, and then remains constant and/or even increases for $T > 1100$ K. The decrease is ascribed to a reduction in the ionic short-range order and the increase to its enhancement. Similarly, in Se_c–Te_{1-c} liquid alloys, Takeda *et al* (1985) observed a Schottky-like excess heat capacity which attains a maximum value of about 30 J mol^{-1} K^{-1} for $c = 0.4$. The change of the average coordination number from 2 to 3 with increasing temperature is responsible for

0953-8984/95/254803+18$19.50

this behaviour. Finally, in the metal–molten-salt system Bi–BiI_3, Ichikawa (1984) found that the excess heat capacity takes large values of 100 to 120 J mol^{-1} K^{-1} over a broad composition range (up to 50% Bi in BiI_3), resulting from the presence of large covalently bonded Bi polycations.

The question of the stability of the Zintl ions upon melting is intimately related to the charge transfer, which is mainly responsible for the formation of complex ionic arrangements. The alkali–tin alloys are good candidates for studying the charge transfer since the smaller size of Sn and its large electronegativity lead one to expect that the corresponding Sn_4^{4-} would be more stable than Pb_4^{4-}. This trend has been confirmed by the results of electrical resistivity measurements for alkali–lead alloys (van der Lugt and Geertsma 1987), and for alkali–tin alloys (Xu *et al* 1992). The structural results obtained by neutron diffraction on NaSn, KSn, and CsSn provide evidence for the presence of Sn_4^{4-} in the liquid and suggest that they are more stable than the corresponding Pb_4^{4-} (Reijers *et al* 1990).

In this paper we report the first comprehensive and complete interpretation of the heat capacity of these alloys. The experimental details of the specific heat of liquid alkali–tin alloys will be published in a separate paper (Johnson *et al* 1995). The dependence of the heat capacity upon temperature is determined accurately and analysed using a model based on a dissociation scheme of the Zintl ions with temperature. The model leads to an estimate of the relative concentration of M_4^{4-}, the free M and alkali ions.

2. Theory

Consider one mole of the liquid alloy system A_cM_{1-c} (A = alkali, M = group IV element). We assume that the one mole of liquid is formed of c moles of A, $(1-z)(1-c)/4$ mol M_4^{4-} and $z(1-c)$ mol M, where z is the degree of dissociation of the clusters. The binding energy, E_c, defined by the reaction

$$M_4^{4-} \rightleftharpoons 4M + E_c \tag{2.1}$$

depends on temperature and composition and z: $E_c = E_c^0 + E_c^1 z + \cdots$. Following Akdeniz and Tosi (1987), the total free energy of this system is

$$F = E_{cluster} - TS_m + F_{hs} + F_{Coul} + F_{tr} + F_{rot} + F_{vibr} \tag{2.2}$$

where $E_{cluster} = -(1-c)(1-z)/4E_c$. The configurational entropy, S_m, is approximated by an ideal random distribution of different particles (ions and clusters):

$$\begin{aligned} S_m = -k_B[&(1-c)(1-z)/4\ln(1-c)(1-z)/4 + c\ln c \\ &+z(1-c)\ln z(1-c) - (1+3c+3z(1-c))/4]. \end{aligned} \tag{2.3}$$

The terms $F_{hs} + F_{Coul}$ are contributions to the free energy from the approximation of the particles as charged hard spheres: they represent the medium contribution. Changes in the free energy due to changes in the number of free electrons are not taken into account, except in so far as in E_c. The remaining three terms F_{tr}, F_{rot}, and F_{vibr} are the translational, rotational, and vibrational contributions to the free energy, respectively. Classical ideal solution expressions can be used to define F_{tr} and F_{rot} (Moore 1968). For F_{vibr}, one has only to include the contribution of the clusters; we approximate, unless specified otherwise, the vibrational spectrum of the tetrahedron by one characteristic frequency ω_c. So at high temperatures ($\hbar\omega_c \ll k_BT$), the vibrational partition function becomes

$$z_{vibr} = (k_BT/\hbar\omega_c)^6 \tag{2.4}$$

where the exponent is the total number of degrees of vibrational freedom $d_v = 6$.

The degree of dissociation z is obtained from minimization of F with respect to z. One finds

$$\frac{(4z)^4}{(1-z)} = A_M T^{-3}(4/(1-c))^3 \exp[-(E_c + E_{ex} - (1-z)\,\delta E_c/\delta z)/k_B T]. \tag{2.5}$$

This equation is similar to the usual law of mass action. The pre-exponential factor, A_M, is

$$A_M = A_M^0(\hbar\omega_c/k_B)^6 \ (\mathrm{K}^3) \tag{2.6}$$

where

$$A_M^0 = \Omega^3\lambda^6\pi\sigma_r m_M^6/(m_c^{3/2}(2\pi)^3(ABCN_{Av}^3)^{1/2}) \ (\mathrm{K}^{-3}) \tag{2.7}$$

and

$$E_{ex} = 4/(1-c)\,\delta(F_{hs} + F_{Coul})/\delta z \tag{2.8}$$

where m_c is the molecular cluster mass and Ω the average atomic volume, m_M the atomic weight of M, and A, B and C are the moments of inertia; σ_r is the number of rigid rotations of the molecule, and $\lambda = (k_B/(2\pi\hbar^2 N_{Av}))^{1/2} = 5.729\times10^{-2}$ mol$^{1/2}$ g$^{-1/2}$ K$^{-1/2}$ Å^{-1}. This quantity (E_{ex}) is the change in the free energy of the liquid due to the dissociation of the clusters. It is the liquid lattice potential at the position of the cluster. Via this term any ion/particle can influence the equilibrium, i.e. the degree of dissociation. Using the mean-spherical approximation (MSA) for the charged hard-sphere contribution one can show, numerically, that E_{ex} is only weakly dependent on the degree of dissociation (see Akdeniz and Tosi (1987, 1990)). So, just as for the bare binding energy of the cluster, we assume that $E_{ex} = E_{ex}^0 + zE_{ex}^1$, and define an effective binding energy of the cluster as appearing in the exponential of equation (2.5):

$$E_B = E_c - (1-z)E_c^1 + E_{ex} = E_0 + zE_1 \tag{2.9}$$

so that $E_0 = E_c^0 - E_c^1 + E_{ex}^0$ and $E_1 = 2E_c^1 + E_{ex}^1$ (see table 1).

Table 1. The binding energy (eV) of Sn_4^{4-} and Pb_4^{4-} tetrahedra (a) derived from the best fit to specific heat data (see the text and table 4), (b) derived from lattice energy differences (taken from von Schnering 1981) and (c) as calculated within a simple Hückel scheme (Geertsma 1995).

Case:	KSn	RbSn	CsSn	KPb	RbPb	CsPb
a	1.8	2.0	2.0	1.6	1.5[5]	1.7
b	1.7	1.80	1.97	1.40	1.54	1.67
c	5.70	5.70	5.70	3.90	3.90	3.90

We will treat the temperature-independent part of the pre-exponential factor (A_M) and the effective binding energies (E_0, and E_1) as fitting parameters to the experimental data. The pre-exponential factor, excluding the vibrational part, A_M^0, can be calculated, and its values for the various systems are grouped in table 2.

Taking into account the influence of the liquid medium and of the translational, rotational and vibrational degrees of freedom we get for the specific heat (see appendix A for details of the derivation):

$$C^e = R\frac{(1-c)}{4}z(1-z)\frac{[3-D+(E_0+zE_1)/k_BT - (\delta E_{ex}/\delta T)/k_B]^2}{4-3z+z(1-z)E_1/k_BT}$$
$$-T\delta^2 F_{Coul}/\delta T^2 + R\frac{1-c}{4}[(1-z)(3-D) + 3/2(4z+c)] \tag{2.10}$$

Table 2. The pre-exponential factor $A_M^0 = (\Omega m_M/R_{MM})^3 \times 3.65 \times 10^{-10}$ mol^3 K^{-3}; m_M is the atomic mass of M, Ω is the average atomic volume. The values in parenthesis are calculated using the following approximation for the average atomic volume of NaSn-type compounds: $\Omega = (50/32)(R_{AM}^{ion})^3$, where R_{AM}^{ion} is the sum of the univalent atomic radii taken from Pauling (1960). The average atomic volumes Ω and interatomic distances in the tetrahedra R_{MM} are from Reijers (1990). Note that this factor has still to be multiplied by $(\hbar\omega_c/k_B)^6$ to get A_M (equation (2.6)).

	NaSn	KSn	RbSn	CsSn	NaPb	KPb	RbPb	CsPb
A_M^0	—	15.19	—	31.71	28.8	68.88	97.68	145.52
(2.17)	(7.94)	(12.64)	(22.08)	(14.56)	(54.40)	(82.80)	(140.00)	
Ω (Å^3)	—	43.5	—	55.6	32.5	46.1	52.1	59.5
R_{AM} (Å)	2.40	2.82	2.97	3.16	2.55	3.01	3.16	3.35
R_{MM} (Å)	2.83	2.98	2.98	2.98	3.14	3.33	3.35	3.35

where

$$D = \mathrm{d}\ln Z_{vib}/\mathrm{d}T = \sum_i d_i(\hbar\omega_i/k_BT)\exp(\hbar\omega_i/k_BT)/[1-\exp(-\hbar\omega_i/k_BT)]^{d_i}.$$

For $\hbar\omega_i \ll k_BT$, which is the case in this work, $D = 6$, the number of degrees of freedom of vibration of the tetrahedron ($d_v = 6$). The specific heat depends on $\delta E_{ex}/\delta z$ via a term in the denominator of equation (A16), which does not appear in the equilibrium equation (equation (2.5)). It is impossible to separate the bare cluster binding energy E_c^0 from the medium contributions (E_{ex} and E_c^1). The first term in equation (2.10) is due to the dissociation of the tetrahedra ($\mathrm{d}z/\mathrm{d}T$), and the second term arises from the change in contribution of the various degrees of freedom of the alloy components. The last term gives an appreciable but nearly temperature-independent contribution to the specific heat. Since the dissociation of the tetrahedra is occurring over a relatively small temperature range of the order of 400 K, the change in degree of dissociation (z) is large, and the first term gives the largest contribution to C^e. It will show up as a peak, or *Schottky-like anomaly*, in the heat capacity.

One can show numerically, using the MSA, that $\delta E_{ex}/\delta T$ is small, and negligible w.r.t. E_c/k_BT. Similarly, $\delta E_{ex}/\delta z$, which can be either positive or negative, is small if we assume that the packing fraction does not vary with the degree of dissociation.

2.1. Analytical analysis of the specific heat data

The maximum in the heat capacity occurs at T_{max} when approximately half of the clusters are dissociated ($z \approx 1/2$). Thus one can write for E_B:

$$\frac{E_B}{k_BT_{max}} = \ln A_M + \ln 2 - 3\ln(1-c) - 3\ln T_{max} \tag{2.11}$$

where $E_B = E_0 + E_1/2$. When E_B increases and A_M is constant, T_{max} is expected to increase, i.e. the maximum value of the heat capacity occurs at higher temperatures when the binding energy increases. When A_M increases and E_B remains constant, T_{max} should decrease.

From equation (2.11) we derive the maximum value of the heat capacity:

$$C_{max}^e = \frac{R}{80}\frac{[E_B/k_BT_{max}) - 3]^2}{1 + 0.1E_1/k_BT}. \tag{2.12}$$

The value of C_{max}^e increases with the ratio E_B/k_BT_{max}.

We now proceed to calculate the parameters of this model, assuming that the binding energy does not depend on the degree of dissociation. We also neglect, for simplicity, the last term of equation (2.10). This will result in a small overestimate of the binding energy. A_M and E_B can be calculated by using the experimental value of T_{max}. Such a procedure applies only to the stannides, where a maximum is observed.

The results in table 3 show that the binding energy of Sn_4 are nearly independent of the alkali except for NaSn where an appreciably smaller binding energy is obtained. These values compare well with those determined from lattice data (von Schnering 1981), and are about a factor two smaller when compared with the binding energy of these charged tetrahedra calculated within a simple Hückel scheme (for details: Geertsma 1995).

Table 3. The parameters of the theory are fitted to the analytical expression at the maximum of the heat capacity of ASn compounds. Experimental values are from Sabougi (1995) and Johnson *et al* (1995). ΔT is the width of the Schottky anomaly.

	Na	K	Rb	Cs	
T_{max} (K)	910	1210	1235	1310	Experimental
C^e_{max} (J mol^{-1} K^{-1})	10	42.6	37.4	34.6	Experimental
E_B/k_BT_{max}	12.81	23.24	21.97	21.24	Equation (2.12)
E_B (eV)	1.00	2.42	2.34	2.40	
$\ln A_M$	30.48	41.76	40.55	40.00	Equation (2.11)
A^0_M	2.17	7.94	12.64	22.08	Equation (2.7)
$\bar{\omega}_c$ (meV)	12	64.3	48.6	40.5	Equation (2.6)
ΔT (K)	~400	~250	~350	~400	Experimental

From A_M, we can derive *characteristic* vibrational frequencies of these tetrahedra. The frequency is very small for NaSn (17 meV); it decreases from about 64 meV for KSn to 41 meV for CsSn. We found a similar decrease in the calculated frequency of the breathing mode in the sequence KSi (50 meV), RbSi (43 meV), CsSi (30 meV), for the Si_4A_4 tetrahedra (Geertsma 1995). If a linear dependence of the binding energy on z is assumed, then E_B decreases with z. Fitting to the specific heat maximum, one finds that when this correction to the binding energy increases, a smaller E_B and A_M are needed and consequently a smaller characteristic vibrational frequency is obtained.

Another method is to assign a reasonable value for the characteristic vibrational frequency, i.e. $\hbar\omega = 80$ meV. For RbSn we obtain ($T_{max} = 1210$ K; $A_M = 1.126 \times 10^{18}$):

$$\frac{E_B}{k_BT_{max}} = 44.3 - 3\ln T_{max} = 23.0. \tag{2.13}$$

Similar values are obtained for CsSn and KSn. For the equiatomic alkali tin alloys we find that T_{max} and E_B increase in the sequence: KSn (1170 K, 2.3 eV), RbSn (1210 K, 2.4 eV), CsSn (1310 K, 2.6 eV). Substituting the value found for E_B/k_BT_{max} we find $C^e_{max} = 40.3$ J mol^{-1} K^{-1} remarkably close to the measured values. C^e_{max} for ASn decreases slightly with increasing weight of the alkali, which is in agreement with the model, where for the same sequence A_M increases and the ratio E_B/k_BT_{max} decreases.

In the equiatomic APb systems, the heat capacity decreases strongly and continuously with increasing temperature. One could deduce that the temperature where the maximum in the heat capacity would occur is below the melting point in the metastable subcooled liquid and expect that its value is larger than that of the alkali–tin compounds. This can only be explained within our model if we assume that A_M is slightly larger than for the tin alloys, and that the binding energy of the lead tetrahedra is smaller. It follows that ω_c is nearly

Table 4. Binding energy (E_0, E_1) and pre-exponential ($\ln A_M$) parameters of the model fitted to the experimental curves. The characteristic frequency of the tetrahedron is $\hbar\omega$. The error is defined as the root mean square deviation of the fitted curve from the experimental one. The fits are performed on a set of experimental points with a temperature step of 25 K. The fits for the various compounds are in the following temperature ranges: for KPb: 850–1125; RbPb: 875–1175; CsPb: 925–1200; KSn: 1125–1500; RbSn: 1150–1500; CsSn: 1175–1500 K. For more details see the text.

	$\ln A_M$	E_0 (eV)	E_1 (eV)	$\hbar\omega_c$ (meV)	Error	Remark
KPb	44.6	1.63	0.12	70.7	0.068	Fitted to all temperatures
	42.9	1.62	0	53.3	0.071	Fitted with $E_1 = 0$
	32.0	1.25	−0.43	8.8	0.100	$\hbar\omega_c$ from Price and Saboungi (1991)
	35.9	1.41	−0.30	16.9	0.096	See the previous remark
RbPb	38.3	1.56	−0.17	23.4	0.061	Fitted to all temperatures
	41.3	1.62	0	38.5	0.074	Fitted with $E_1 = 0$
CsPb	39.0	1.69	−0.12	24.6	0.091	Fitted to all temperatures
	39.2	1.68	−0.11	25.4	0.111	Weighted from 975–1100 K (10×)
	41.0	1.73	0	34.3	0.092	Fitted with $E_1 = 0$
	41.1	1.73	0	34.9	0.092	$E_1 = 0$, weighted from 975–1100 K (5×)
	31.5	1.40	−0.54	7.2	0.37	$\hbar\omega_c$ from Price and Saboungi (1991)
	36.9	1.62	−0.25	17.6	0.075	See previous remark
KSn	33.1	1.84	−0.66	14.9	0.130	Fitted to all temperatures
	34.2	1.89	−0.58	17.9	0.177	Weighted from 1175–1250 K (100×)
	40.8	2.27	0	53.8	0.588	$E_1 = 0$, weighted from 1175–1250 K (100×)
RbSn	36.1	2.02	−0.38	22.8	0.017	Fitted to all temperatures
	35.6	1.99	−0.42	20.9	0.045	Weighted from 1175–1300 K (100×)
	39.6	2.16	0	40.8	0.185	$E_1 = 0$, weighted from 1175–1300 K (100×)
CsSn	35.4	2.04	−0.46	18.5	0.110	Fitted to all temperatures
	36.0	2.07	−0.36	20.4	0.150	Weighted from 1250–1350 K (100×)
	39.4	2.30	0	35.9	0.284	$E_1 = 0$, weighted from 1250–1350 K (100×)

the same as that of the tin tetrahedra.

2.2. *Numerical analysis of the specific heat data*

The effective binding energy and the pre-exponential factor were used as primary fitting parameters and determined so that the maxima of the theoretical and experimental curve coincide.

(a) *Alkali plumbides.* We first calculated the variations of the binding energy with temperature for various values of the pre-exponential factor. We neglected E_1 in the denominator of the specific heat (equation (2.10)). Within a nearly temperature-independent binding energy approximation the best fits were obtained for values of A_M corresponding to a characteristic frequency ω_c in the range 30–50 meV, which is similar to those obtained for the alkali stannides. The deviations of ±5% are largest near T_m and in the high-temperature tail of the anomaly. One can improve the fit by introducing a small dependence of the binding energy on z of about −0.17 eV for RbPb and −0.12 eV for CsPb. The remaining deviations can be due to order–disorder phenomena, not considered in our model, occurring just above T_m and in the high-temperature tail of C_P. From these fits we find that, as expected, the binding energy of the Pb_4^{4-} tetrahedra increases slightly from 1.6 eV for KPb

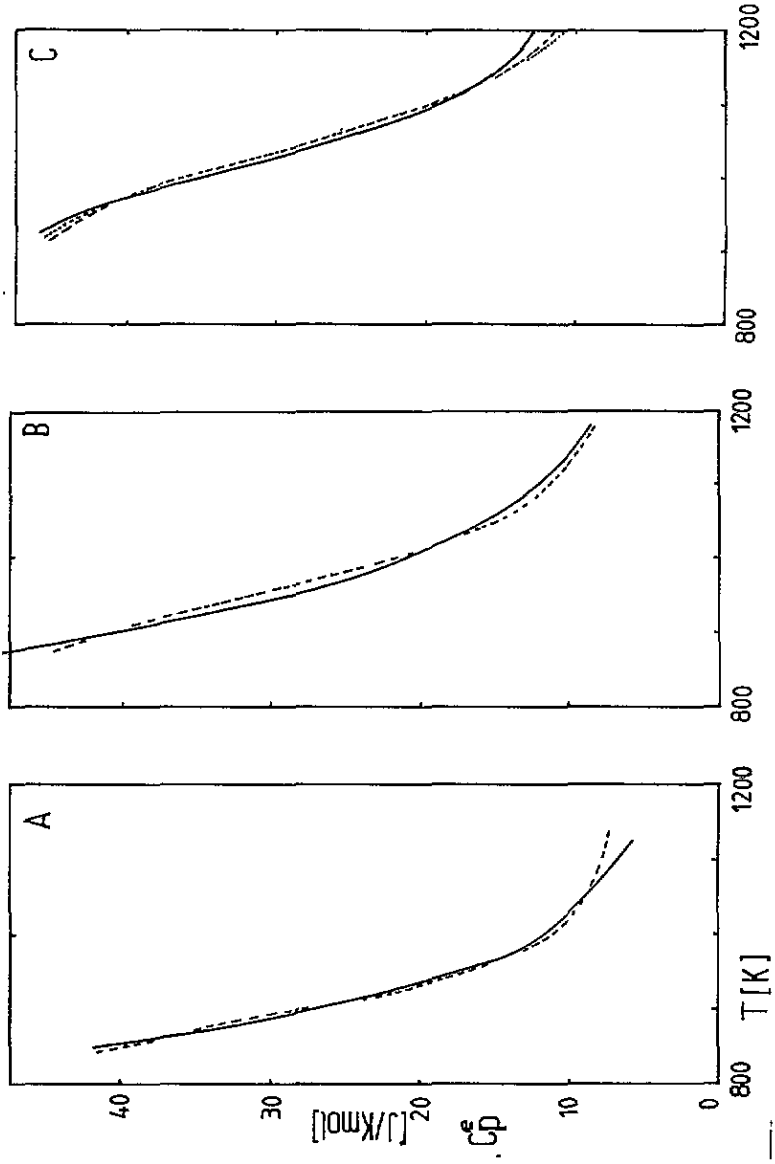

Figure 1. Excess specific heat (C^e) as a function of temperature for the alkali plumbides. The full lines are the experimental excess specific heat. A: $K_{0.5}Pb_{0.5}$: case (a) of figure 2. B: $Rb_{0.5}Pb_{0.5}$: case (a) of figure 2. C: $Cs_{0.5}Pb_{0.5}$: long-dashed case (a); short-dashed case (b) of figure 2. For KPb and RbPb the case (b) (figure 2) is nearly indistinguishable from the experimental curve.

and RbPb to 1.7 eV for CsPb. Finally, the degree of dissociation is very high (see figure 2): 0.8 for KPb, 0.7 for RbPb, 0.65 for CsPb just above T_m, and at 1000 K it is higher, at least 0.9 for KPb and RbPb and 0.8 for CsPb.

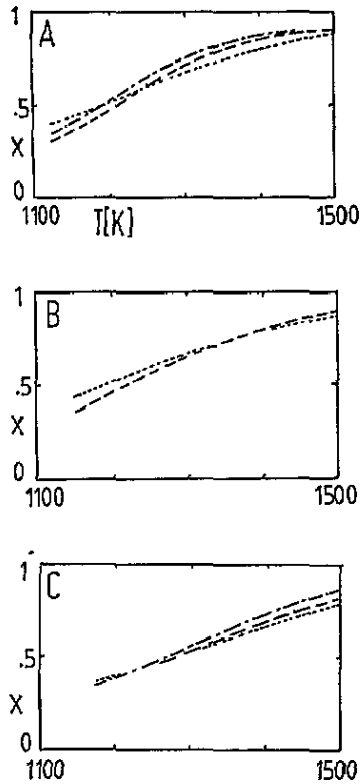

Figure 2. Degree of dissociation (x) as a function of temperature for the alkali plumbides. A: $K_{0.5}Pb_{0.5}$: $\ln A_M = 42.9$, $E_0 = 1.62$ (a); $\ln A_M = 44.6$, $E_0 = 1.63$, $E_1 = 0.12$ (b). B: $Rb_{0.5}Pb_{0.5}$: $\ln A_M = 41.3$, $E_0 = 1.62$ (a); $\ln A_M = 38.3$, $E_0 = 1.56$, $E_1 = -0.17$ (b). C: $Cs_{0.5}Pb_{0.5}$: $\ln A_M = 40.1$, $E_0 = 1.73$ (a); $\ln A_M = 39.0$, $E_0 = 1.69$, $E_1 = -0.12$ (b).

(b) *Alkali stannides.* Following the same procedure as above, we calculated the binding energy as a function of temperature from the specific heat data for various values of A_M. We neglected the E_1-term in the denominator of equation (2.10). For each temperature, two values of the binding energy fit the data and form two separate branches. The lower one usually has a maximum, while the upper has a minimum. The temperature dependence of the binding energy is much larger than for the plumbides. The range of binding energy values of the lower branch is about 0.3 eV. The upper branch increases to rather high values with increasing temperature. The binding energy values are of the same order as obtained above from the analytical solution. In figure 3 we have plotted the experimental and calculated excess specific heat for the alkali stannides. For K, Rb, and Cs, the theoretical curve is above the experimental one: At high temperatures the dissociation is faster than described by the model with constant binding energy. We also fitted the data using a binding energy that depends on z. The results of these fits are shown in figure 3, and the corresponding degrees of dissociation in figure 4. As expected, the binding energy increases slightly from 1.8 eV for KSn to 2.0 eV for CsSn. These binding energies are slightly larger than for the plumbides but the degree of dissociation is smaller and independent—as for the plumbides—of the final model parameters (see figure 4). The vibrational frequencies derived from the pre-exponential factor are slightly smaller than those for the plumbides (see table 4). Overall, the quality of the fits of the stannides is not as good as for the

plumbides. This may result from terms of higher order in the degree of dissociation in the expansion of the binding energy. Note that the first-order binding energy E_1 is much larger than for the plumbides.

(c) *Composition dependence of C_p.* A pronounced peak has been observed near the equiatomic composition in the specific heat of K–Pb and Rb–Pb by Saboungi *et al* (1988). Using the parameter values derived for equiatomic RbPb we have calculated the composition dependence of the specific heat for various temperatures. We found that a composition independent binding energy cannot explain the observed specific heat, because the tetrahedral clusters are most stable at the equiatomic composition. In a tight-binding picture of the bonding of these clusters all bonding and antibonding levels are occupied for A_4M, and so for this composition and in the alkali-poor region, the clusters are unstable. By assuming that the binding energy can take the form

$$E_B = E_{B0} + c(1-c)E_{B1} \tag{2.14}$$

where the parameters are chosen such that E_B vanishes for the A_4M compound, and the binding energy at the equiatomic composition is equal to the one defined earlier in equation (2.9) for $z = 0.5$, so in terms of the binding energy parameters defined above we get: $E_{B0} = -16(E_0 + 0.5\,E_1)/9$ and $E_{B1} = -25E_{B0}/4$. This determines E_{B0} and E_{B1}. For Rb–Pb we have calculated on this basis the specific heat (figure 5), which shows the maximum reported experimentally. The peak decreases with increasing temperature. The fraction of clusters is plotted in figure 6. As expected, it peaks around the equiatomic composition; far from this composition it decreases fast, and for $c > 0.6$ and $c < 0.4$, nearly all clusters have dissociated.

(d) *Discussion.* The ratio of the vibrational frequencies found for tetrahedra by Kliche *et al* (1987), is about: 1 (E):1.33 (T):1.66 (A). This differs appreciably from the ratio $(1{:}\sqrt{2}{:}2)$ that one would obtain when only the bond–stretching force constant is taken into account.

Using this ratio we find that the characteristic frequency is related to the breathing mode frequency of the free tetrahedron by: $\omega_{A_1} = 1.42\omega_c$. The breathing mode vibrational frequencies derived from the pre-exponential (A_M) when fitted to all temperatures (see table 4) are $\hbar\omega_A(Pb_4^{4-}) = 101$ (KPb), 55 (RbPb), 34 (CsPb) meV and $\hbar\omega_A(Sn_4^{4-}) = 21$ (KSn), 32 (RbSn), 27 (CsSn) meV. The values for the breathing mode of the stannides compare well with those found for the isoelectronic Sb_4 ($\hbar\omega_{A_1} \approx 30$ meV) in the gas phase (Kliche *et al* (1987)) although the frequencies of the charged Sn_4^{4-} tetrahedra are somewhat smaller than found for the isoelectronic Sb_4 molecules. A similar trend in the breathing mode frequencies has been found for the solid-state clusters Si_4^{4-} (60 meV) and Ge_4^{4-} (33 meV) compared with their analogous gas-phase P_4 (76 meV) and As_4 (44 meV) respectively (see Bürger and Eujen 1972).

Next let us consider the vibration frequencies of the Pb_4^{4-} tetrahedra. Toukan *et al* (1990) found from a MD study the following breathing mode frequency for Pb_4^{4-}: $\hbar\omega_{A_1} \approx 21$ meV in liquid KPb. This frequency is somewhat higher than found for the isoelectronic Bi_4 tetrahedron ($\hbar\omega_A = 18.6$ meV). From an analysis of inelastic neutron scattering measurements on liquid KPb and CsPb, Price and Saboungi (1991) found 12.5 and 10.2 meV in KPb and CsPb, respectively, for the breathing mode frequencies of the Pb tetrahedron. Recently similar results have been obtained using the Car–Parrinello method on liquid CsPb by de Wijs (1995). He finds a peaked structure in the Pb velocity autocorrelation function extending from 10 meV to 20 meV. This implies that the breathing mode of the Pb tetrahedron is at about 20 meV, in agreement with the findings of Toukan *et al* (1990). The Cs velocity autocorrelation function peaks at a lower energy from 5 to about 15 meV.

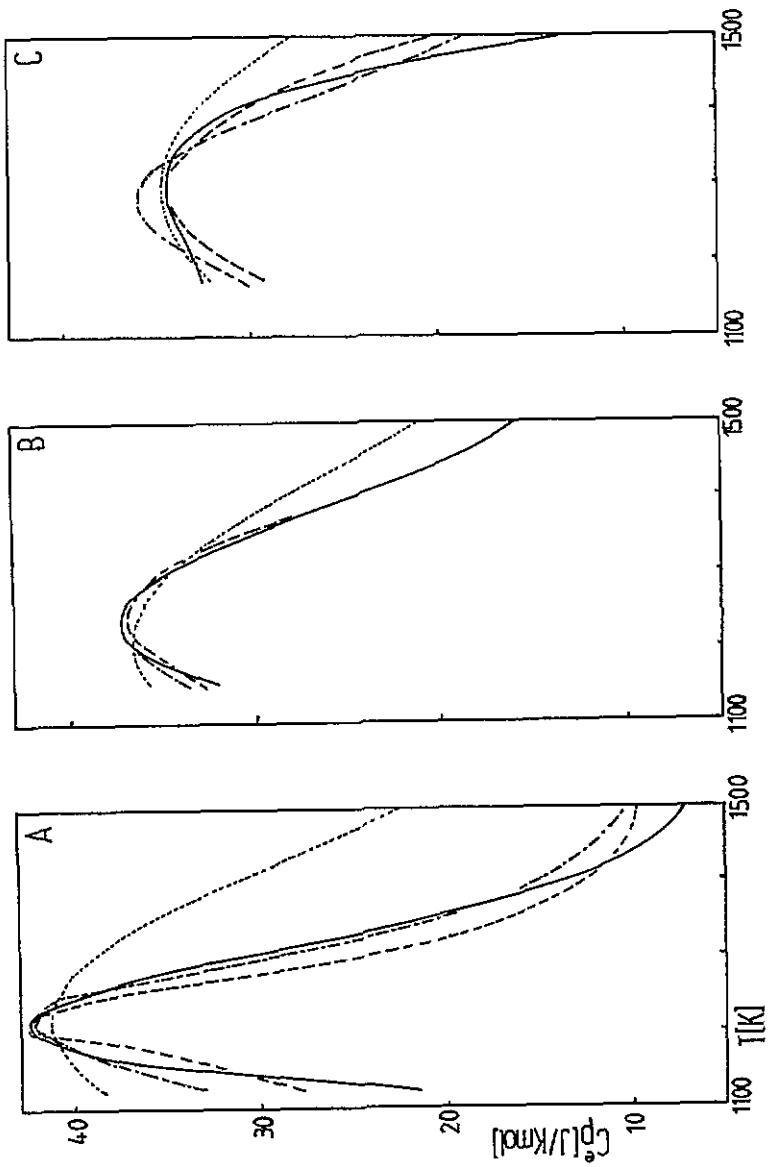

Figure 3. Excess specific heat (C^e) as a function of temperature for the alkali stannides. The full lines are the experimental excess specific heat of these systems. The short-dashed line is the fit to the top, taking binding energy as independent of the degree of dissociation. The long-dashed line is fitted to the top and the dash–dot line is an overall fit. The parameter values are in table 4.

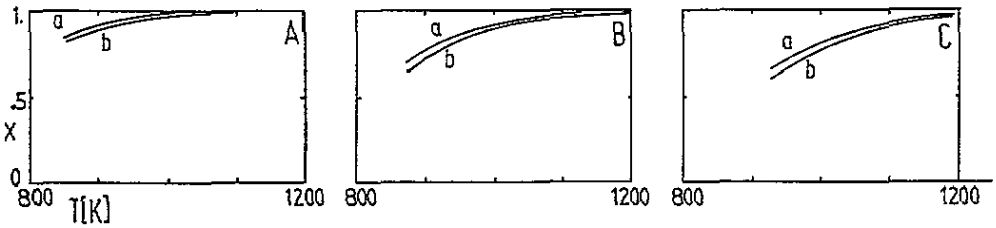

Figure 4. The degree of dissociation (x) as a function of temperature corresponding to the specific heat of figure 3.

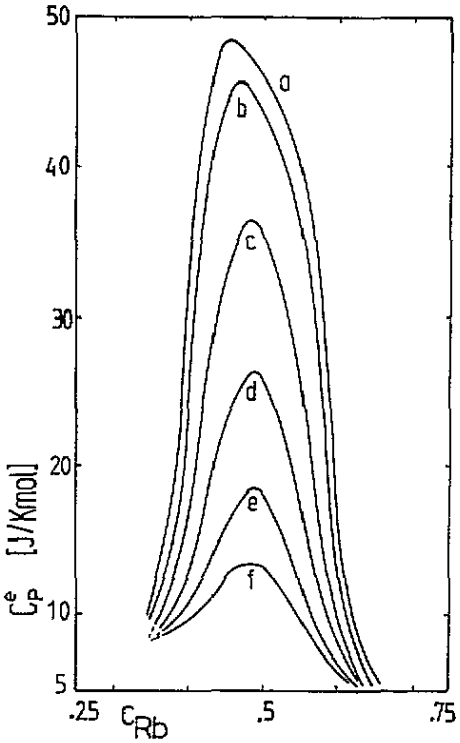

Figure 5. Composition dependence of the specific heat of Rb_cPb_{1-c} for various temperatures: 875 (a), 900 (b), 950 (c), 1000 (d), 1050 (e), 1100 (f). The parameters used are: $\ln A_M = 38.3$, $E_{B0} = -2.66$, $E_{B1} = 16.66$, $E_1 = -0.17$ eV.

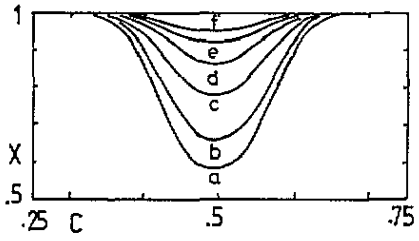

Figure 6. Composition dependence of the degree of dissociation of Rb_cPb_{1-c} for various temperatures: 875 (a), 900 (b), 950 (c), 1000 (d), 1050 (e), 1100 (f). The parameters used are: $\ln A_M = 38.3$, $E_{B0} = -2.66$, $E_{B1} = 16.66$, $E_1 = -0.17$ eV.

We do not have a clear explanation for the difference of nearly a factor of 8 for KPb and nearly a factor of 3 for CsPb between our thermodynamically determined vibrational frequencies and the ones determined from inelastic neutron scattering data. We can, however, make the following remarks. From a close examination of the inelastic neutron data of Price and Saboungi and comparing these with the calculations of de Wijs on CsPb, we conclude that the frequencies, as determined from the neutron data, are the frequencies of the Cs tetrahedron capping the four faces of the Pb tetrahedron. Also, these will have the same frequency ratio as for a normal tetrahedron. At higher energy there are indications for peaks at 14.4, 18.3 and 25 meV, with the ratio 1:1.3:1.7 as expected for a tetrahedron.

So the breathing mode frequency of the Pb tetrahedra derived from inelastic neutron data is about 25 meV instead of 10.2 meV.

What would happen when we fitted the plumbides using the vibrational frequencies determined by inelastic neutron diffraction? With the original interpretation of Price and Saboungi the values of $\ln A_M$ have to be shifted by -10 for KPb and -7 for CsPb relative to the fit to all temperatures in table 4. In the case where one interprets the weak bands at higher energy in the inelastic neutron spectrum as the Pb_4 modes one has to shift the pre-exponential factor by -8.5 for KPb and -2 for CsPb. In order to get a decent fit one has to take a smaller value for the binding energy than that given in table 4 (see below equation (2.11)). The results of the fits based on these vibration frequencies are in table 4. In order to get a good fit it is essential to take into account the dissociation dependence of the binding energy. Note the large error in the case of CsPb when we use the vibrational frequencies from the low-energy interpretation of the inelastic neutron spectrum.

The small increase in stability of the Pb tetrahedra with the heavier alkali is as we expected. Also the difference of the stability of the Sn and Pb tetrahedra of about 0.3 to 0.5 eV is as expected.

Note that when we assume that T_{max} does not change much by changing the binding energy, one can derive from equation (2.11) and the fitted parameters in table 4 the change in E_0 due to changes in $\ln A_M$. In the case where we use the high-energy interpretation for the vibrational spectra, one calculates for KPb ($T_{max} = 720$ K) a change in E_0 of -0.42, and for CsPb ($T_{max} = 900$ K) a change in E_0 of -0.23 eV, which gives for both KPb and CsPb a binding energy, E_B (see equation (2.11)), of about 1.2 for KPb and 1.46 eV for CsPb. So these analytical expressions give a good indication of the magnitude of the binding energy E_0.

We also have to mention the possibility of larger 3D networks of threefold-coordinated Pb_n. Such a structure has been found in the reverse Monte Carlo analysis of KPb (McGreevy 1995) and the simulations of de Wijs (1995) on CsPb. In the latter one also finds clear indications for isolated Pb tetrahedra. In our model the structure of the background medium in which the tetrahedrons are immersed is rather irrelevant. The binding energy of the tetrahedron we find is, obviously, with respect to this background. Whether there is still some bonding between the Pb/Sn ions is included in E_B.

From the discussion at the end of the previous section we conclude that this model is even able to predict the vibrational frequencies when the maximum of the Schottky anomaly is above the melting temperature. The other way around would be to calculate from equation (2.11), using known vibrational frequencies, the pre-exponential factor, and from this the temperature where the Schottky anomaly has its maximum. The binding energy could be found by some reasonable extrapolation of the stannides and plumbides to the germanides and silicides. In order to be able to observe temperature corresponding to the maximum (T_{max}) in the Schottky anomaly, the binding energy E_B has to be larger than $E_B(T_{melt})$. In order to get the maximum 300 K above the melting temperature of the alkali germanides (Moffat 1984) the binding energy is: for NaGe 1.9, for KGe 2.0, for RbGe 1.9, and for CsGe 1.8 eV. These values for the binding energy, which are the minimum values required to push the Schottky anomaly above the melting temperature, are somewhat smaller than the binding energies one expects for Ge_4^{4-}. So for the alkali germanides we expect the Schottky anomaly far above the melting point. For example, taking a reasonable value for the binding energy of the germanide tetrahedron of 2.5 eV, we obtain maxima of the Schottky anomaly at 2600, 2270, 2160, 2050 K for the Na, K, Rb and Cs germanide respectively.

(e) *The Darken stability function.* Finally, the excess stability (Darken 1967), which is a measure of the thermodynamic rigidity of the system, has been evaluated within this

model; see appendix 3. There are three contributions due to (i) the salt-like medium; (ii) the dependence of the binding energy on the degree of dissociation; and (iii) the dissociation of the clusters. The latter gives a negative contribution to the excess stability, and has a minimum at nearly the same temperature as where the excess specific heat has a maximum. This minimum becomes especially deep when the specific heat maximum is large, and when there is a strong coupling between cluster and medium as represented by E_{ex}. In such a case large fluctuations in the composition are possible. This probably explains the unexpectedly small value of the excess stability found for the equiatomic alkali plumbides by Tumidajski *et al* (1990).

3. Conclusions

The experimental heat capacities were determined at constant pressure, while the theoretical ones are calculated at constant volume.

The experimental specific heat decreases much more quickly with temperature than predicted by the model with a constant binding energy. We can explain this fast decrease of the specific heat by assuming that the effective binding energy (E_B) depends on the degree of dissociation (z). When taking this into account we obtain much better fits, and we find that the effective binding energy of the tetrahedra decreases with increasing degree of dissociation. Such a decrease in binding energy with degree of dissociation is not unlikely, because of the fact that the medium becomes more metallic when the dissociation degree increases, screening the liquid lattice potential and slightly destabilizing the tetrahedra. The fits of the plumbides are of a better quality than those of the stannides. This is probably due to fact that for the plumbides one fits only to the high-temperature tail of the Schottky anomaly, while for the stannides one has to fit over the entire anomaly. The effective binding energies found from these numerical fits are (for $z = 0$): $E_0(Pb_4^{4-}) = 1.65 \pm 0.1$ eV and $E_0(Sn_4^{4-}) = 2.0 \pm 0.2$ eV.

The binding energy increases slightly in the sequence K, Rb, Cs, in agreement with the model proposed by Geertsma *et al* (1984). When relatively stable intermediate clusters, like pairs or triplets, are present, then one would expect a broadening of the specific heat peak. This is clearly not observed in the plumbides. In the stannides, a higher degree of anion association than into only tetrahedra can be one of the causes of the deviation between our model and the experimental data. Higher associates can give a faster decrease of the specific heat, assuming that the intermediates of the dissociation are relatively less stable.

Acknowledgments

The work performed at Argonne National Laboratory was supported by US-DOE, Division of Materials Sciences, Office of Basic Energy Sciences, under Contract W-31-109-ENG-38

Appendix A. The general specific heat expression

Write for the free energy:

$$F = \sum_i [x_i E_i + RTx_i(\ln x_i N - 1) - RTx_i \ln Z_i] + G(\{x_i\}, T) \qquad \text{(A1)}$$

where $G(\{x_i\}, T)$ contains the influence of the medium on the non-interacting particles i. The equilibrium condition is $\delta F/\delta z = 0$. The coefficient of z in x_i is n_i: $(\delta x_i/\delta z) = n_i$.

$$\frac{\delta F}{\delta z} = \sum_i \left[x_i \frac{\delta E_i}{\delta z} + E_i \frac{\delta x_i}{\delta z} + RT \left(\frac{\delta x_i}{\delta z} \ln x_i N - \frac{\delta x_i}{\delta z} \ln Z_i - x_i \frac{\delta \ln Z_i}{\delta z} \right) \right] + \frac{\delta G}{\delta z}. \tag{A2}$$

The equilibrium condition at constant temperature becomes:

$$\sum_i n_i (E_i + RT(\ln x_i N - \ln Z_i)) = -\sum_i x_i \left(\frac{\delta E_i}{\delta z} \right)_T - \left(\frac{\delta G}{\delta z} \right)_T. \tag{A3}$$

The specific heat is given by

$$C_P = -T \frac{\delta^2 F}{\delta T^2}. \tag{A4}$$

Let us first calculate $\delta F/\delta T$:

$$\frac{\delta F}{\delta T} = \sum_i \left(E_i \frac{\delta x_i}{\delta T} + x_i \frac{\delta E_i}{\delta T} \right) + \frac{\delta G}{\delta T} + R \sum_i x_i (\ln x_i N - 1 - \ln Z_i)$$
$$+ RT \sum_i \frac{\delta x_i}{\delta T} (\ln x_i N - 1 - \ln Z_i) + RT \sum_i x_i \left(\frac{\delta x_i}{\delta T} \frac{1}{x_i} - \frac{\delta \ln Z_i}{\delta T} \right). \tag{A5}$$

After some rearrangements using equation (A1) this can be written as:

$$\frac{\delta F}{\delta T} = \left[\sum_i \left(n_i (E_i + RT(\ln x_i N - \ln Z_i)) + x_i \left(\frac{\delta E_i}{\delta z} \right)_T \right) + \left(\frac{\delta G}{\delta z} \right)_T \right] \frac{\delta z}{\delta T}$$
$$+ \left(\frac{\delta G}{\delta T} \right)_z + \frac{F}{T} - \frac{1}{T} \left(G + \sum_i x_i E_i \right) + \sum_i x_i \left(\left(\frac{\delta E_i}{\delta T} \right)_z - RT \frac{\delta \ln Z_i}{\delta T} \right). \tag{A6}$$

The first term vanishes when the system is in equilibrium. Also the temperature derivative of the first term vanishes under equilibrium conditions. Next we have to calculate $\delta^2 F/\delta T^2$. Define for convenience $B = (\delta G/\delta T)_z$, $A_i = (\delta E_i/\delta T)_z$; $Q_i = \delta \ln Z_i/\delta T$. We get

$$\frac{\delta^2 F}{\delta T^2} = \frac{\delta B}{\delta T} + \sum_i \left(A_i \frac{\delta x_i}{\delta T} + x_i \frac{\delta A_i}{\delta T} - x_i R Q_i - RT x_i \frac{\delta Q_i}{\delta T} \right)$$
$$- \frac{1}{T} \left(\frac{\delta G}{\delta z} \right)_T \frac{\delta z}{\delta T} - \frac{1}{T} \sum_i \frac{\delta x_i}{\delta T} E_i - \frac{1}{T} \sum_i x_i \left(\frac{\delta E_i}{\delta z} \right)_T \frac{\delta z}{\delta T} - R \sum_i x_i \frac{\delta \ln Z_i}{\delta T}$$
$$- RT \sum_i \frac{\delta \ln Z_i}{\delta T} \frac{\delta x_i}{\delta T}. \tag{A7}$$

Use

$$\frac{\delta B}{\delta T} = \left(\frac{\delta B}{\delta T} \right)_z + \left(\frac{\delta B}{\delta z} \right)_T \frac{\delta z}{\delta T} \tag{A8}$$

and similar for $(\delta A_i/\delta T)$. This equation can then further be written as

$$\frac{\delta^2 F}{\delta T^2} = \left(\frac{\delta^2 G}{\delta T^2} \right)_z + \sum_i x_i \left(\left(\frac{\delta A_i}{\delta T} \right)_z - 2RQ_i - RT \frac{\delta Q_i}{\delta T} \right)$$
$$+ \frac{\delta z}{\delta T} \left[\sum_i \left(n_i A_i - \frac{1}{T} n_i E_i - \frac{x_i}{T} \left(\frac{\delta E_i}{\delta z} \right)_T - RT n_i Q_i + x_i \left(\frac{\delta A_i}{\delta z} \right)_T \right) \right.$$
$$\left. - \frac{1}{T} \left(\frac{\delta G}{\delta z} \right)_T + \left(\frac{\delta^2 G}{\delta z^2} \right)_T \right]. \tag{A9}$$

From the equilibrium equation we can derive an expression for $(\delta z/\delta T)$:

$$\sum_i n_i \left(\frac{\delta E_i}{\delta T} + R(\ln x_i N - \ln Z_i) + \frac{RT}{x_i}\frac{\delta x_i}{\delta T} - RT\frac{\delta \ln Z_i}{\delta T} \right)$$
$$= -\sum_i \left(\frac{\delta x_i}{\delta T}\left(\frac{\delta E_i}{\delta z}\right)_T - x_i \frac{\delta^2 E_i}{\delta z \delta T} \right) - \frac{\delta^2 G}{\delta z \delta T}. \tag{A10}$$

This can be solved for $\delta z/\delta T$:

$$\frac{\delta z}{\delta T} = -\left(\sum_i \left[n_i (A_i + R(\ln x_i N - \ln Z_i) - RT\frac{\delta \ln Z_i}{\delta T} - x_i \frac{\delta^2 E_i}{\delta z \delta T} \right] - \frac{\delta^2 G}{\delta z \delta T} \right)$$
$$\times \left(\sum_i \left[2n_i \left(\frac{\delta E_i}{\delta z}\right)_T + RT\frac{n_i^2}{x_i} + x_i \left(\frac{\delta^2 E_i}{\delta z^2}\right)_T \right] + \left(\frac{\delta^2 G}{\delta z^2}\right)_T \right)^{-1}. \tag{A11}$$

Now note that the numerator is the same as the coefficient of $\delta z/\delta T$ in equation (A9). So finally we get for the specific heat

$$C_P = -T\left[\left(\frac{\delta^2 G}{\delta T^2}\right)_z + \sum_i x_i \left(\left(\frac{\delta^2 E_i}{\delta T^2}\right)_z - 2RQ_i - RT\frac{\delta Q_i}{\delta T} \right) \right] + T\left[\sum_i \left(n_i \left(\frac{\delta E_i}{\delta T}\right)_z \right.\right.$$
$$\left. - \frac{1}{T} n_i E_i - \frac{x_i}{T}\left(\frac{\delta E_i}{\delta z}\right)_T + x_i \frac{\delta^2 E_i}{\delta z \delta T} - RT n_i Q_i \right) + T\left(\frac{\delta(\delta G/\delta z)_T/T}{\delta T} \right)_z \Bigg]^2$$
$$\times \left[\sum_i \left(2n_i \left(\frac{\delta E_i}{\delta z}\right)_T + x_i \left(\frac{\delta^2 E_i}{\delta z^2}\right)_T + RT\frac{n_i^2}{x_i} \right) + \left(\frac{\delta^2 G}{\delta z^2}\right)_T \right]^{-1}. \tag{A12}$$

Some of the terms can be evaluated at high temperatures:

$$Q_i = \frac{1}{T}(d_{v,i} + d_{r,i} + 3/2) \tag{A13}$$

and

$$2Q_i + T\frac{\delta Q_i}{\delta T} = \frac{d_{v,i} + d_{r,i} + 3/2}{T} \tag{A14}$$

where the factor 3 comes from the translational degrees of freedom of particle i; $d_{v,i} = \delta \ln Z_{vibr}(i)/\delta T$ is the number of vibrational degrees of freedom.

When we neglect the second derivatives except $\partial^2 G/\partial z^2$ in the numerator in the evaluation of the specific heat we get

$$C_P = R\sum_i x_i (d_{v,i} + d_{r,i} + 3/2)$$
$$+ R\left[\sum_i \left(\frac{n_i E_i}{RT} + n_i(d_i + 3) + \frac{x_i}{RT}\frac{\delta E_i}{\delta z} \right) + \frac{1}{RT}\left(\frac{\delta G}{\delta z}\right)_T \right]^2$$
$$\times \left[\sum_i \frac{n_i^2}{x_i} + \frac{2n_i}{RT}\left(\frac{\delta E_i}{\delta z}\right)_T + \frac{1}{RT}\left(\frac{\delta^2 G}{\delta z^2}\right)_T \right]^{-1}. \tag{A15}$$

For the tetrahedral equilibrium we have (subscript 1 is cluster, 2 is metal): $n_1 = -(1-c)/4$ and $n_2 = 1 - c$. Furthermore define the excess binding energy (see equation (2.8)) $E_{ex} = 4/(1-c)(\delta G/\delta z)_T$. We expand the cluster binding energy (see below equation (2.1)) $E_c = E_c^0 + zE_c^1$, and and excess binding energy $E_{ex} = E_{ex}^0 + zE_{ex}^1$. Note that there is a change in sign for the cluster binding energy as defined in this appendix and used in

the main text. Let us define an effective binding energy $E_B = E_c - (1-z)E_c^1 + E_{ex}$ and write $E_B = E_0 + zE_1$, $E_0 = E_c^0 + E_{ex}^0 - E_c^1$, and $E_1 = 2E_c^1 + E_{ex}^1$. The expression for the specific heat can now be written as

$$C_P = R\sum_i x_i(d_{v,i} + d_{r,i} + 3/2) + R\frac{(1-c)}{4}z(1-z)\frac{\left[(E_0 + zE_1)/k_BT + 3 - D\right]^2}{4 - 3z + z(1-z)E_1/k_BT}. \tag{A16}$$

This or a simplified expression is used in the main text. Note two points about this expression. (i) If E_1 becomes very negative, this contribution to the specific heat becomes negative. In this case the approximate expansion of the binding energies breaks down. Note that the prefactor of E_1 in the denominator is $z(1-z)$, so when E_1 is negative but small this contribution to the specific heat has a maximum for approximately $z = 0.5$. (ii) The prefactor of the last term of (A16) is also $z(1-z)$ and so this contribution attains its maximum for $z = 0.5$. This is also the approximate value of the degree of dissociation for which the specific heat has a maximum. The composition dependence of the numerator is small. The numerator determines the magnitude of the maximum of the specific heat. This property can be used in the case where one observes a maximum in the specific heat. This *ansatz* is used in the main text to analyse the specific heat data.

Appendix B. The Darken stability function

Within the same spirit we can derive the Darken stability function (Darken 1967):

$$D = \frac{\delta^2 F}{\delta c^2} \tag{B1}$$

where the free energy F is given by equation (A1). This function is closely related to the concentration fluctuations correlation function, given by

$$S_{cc} = NRT/D. \tag{B2}$$

A straightforward calculation gives for the Darken stability function

$$\begin{aligned}\frac{\delta^2 F}{\delta c^2} = \frac{\delta^2 G}{\delta c^2} &+ \sum_i \left[2c_i\left(\frac{\delta E_i}{\delta c}\right)_z + x_i\left(\frac{\delta^2 E_i}{\delta c^2}\right)_z + RT\frac{c_i^2}{x_i}\right] \\ &+ \frac{\delta z}{\delta c}\sum_i a_i\left[E_i + RT\ln x_i N - RT\ln Z_i\right] \\ &+ \frac{\delta z}{\delta c}\left\{\sum_i\left[c_i\left(\frac{\delta E_i}{\delta z}\right)_c + n_i\left(\frac{\delta E_i}{\delta c}\right)_z + x_i\frac{\delta^2 E_i}{\delta z\,\delta c} + RT\frac{c_i n_i}{x_i}\right] + \frac{\delta^2 G}{\delta z\,\delta c}\right\}\end{aligned} \tag{B3}$$

with $c_i = \partial x_i/\partial c$, and $a_i = \partial^2 x_i/\partial c\,\partial z$. The derivative $(\delta z/\delta c)$ has to be calculated along the equilibrium line. An evaluation gives

$$\begin{aligned}\frac{\delta z}{\delta c} = -&\left\{\sum_i\left[c_i\left(\frac{\delta E_i}{\delta z}\right)_c + n_i\left(\frac{\delta E_i}{\delta c}\right)_z + x_i\frac{\delta^2 E_i}{\delta z\delta c} + RT\frac{c_i n_i}{x_i}\right.\right. \\ &\left.\left. + a_i\left(E_i + RT\ln x_i N - RT\ln Z_i\right)\right] + \frac{\delta^2 G}{\delta z\delta c}\right\} \\ &\times\left[\sum_i\left(2n_i\left(\frac{\delta E_i}{\delta z}\right)_c + x_i\left(\frac{\delta^2 E_i}{\delta z^2}\right)_c + RT\frac{n_i^2}{x_i}\right) + \left(\frac{\delta^2 G}{\delta z^2}\right)_c\right]^{-1}.\end{aligned} \tag{B4}$$

Note that the denominator of this expression is equal to that of the derivative $(\delta z/\delta T)$ derived for the specific heat. The numerator of the last equation is equal to the coefficient of $(\delta z/\delta c)$ in equation (B3). All together we get for the Darken stability function

$$D = \frac{\delta^2 G}{\delta c^2} + \sum_i \left[2c_i \left(\frac{\delta E_i}{\delta c} \right)_z + x_i \left(\frac{\delta^2 E_i}{\delta c^2} \right)_z + RT \frac{c_i^2}{x_i} \right]$$
$$- \left[\sum_i \left(c_i \left(\frac{\delta E_i}{\delta z} \right)_c + n_i \left(\frac{\delta E_i}{\delta c} \right)_z + x_i \frac{\delta^2 E_i}{\delta c \delta z} + RT \frac{c_i n_i}{x_i} \right.\right.$$
$$\left.\left. + a_i (E_i + RT \ln x_i N - RT \ln Z_i)) + \frac{\delta^2 G}{\delta c \delta z} \right]^2$$
$$\times \left[\sum_i \left(2n_i \left(\frac{\delta E_i}{\delta z} \right)_c + x_i \left(\frac{\delta^2 E_i}{\delta z^2} \right)_c + RT \frac{n_i^2}{x_i} \right) + \left(\frac{\delta^2 G}{\delta z^2} \right)_c \right]^{-1}. \tag{B5}$$

The first term of this equation for the Darken stability function is the contribution of the (salt-like) medium and can be rather large around a salt-like composition: the concentration fluctuations are small. The last term is due to the fluctuations coming from the chemical equilibrium, in our case the dissociation of the clusters. This introduces an instability in the system. Note that when the specific heat is large due to a small denominator—which can be due to a large composition dependence of the binding energy E_i—the Darken stability function decreases.

Note that the Darken stability function and the specific heat are related:

$$\frac{\delta^2 D}{\delta T^2} = -\frac{1}{T} \frac{\delta^2 C_P}{\delta c^2}. \tag{B6}$$

When the specific heat is plotted as a function of composition at constant temperature T_0, the composition with zero curvature is c_0; then, when the Darken stability function is plotted as a function of temperature at constant composition c_0, the zero curvature has to appear for T_0.

References

Akdeniz Z and Tosi M P 1987 *Phys. Chem. Liq.* **17** 91–104
——1990 *J. Non-Cryst. Solids* **117/118** 692–5
Bürger H and Eujen R 1972 *Z. Anorg. Allg. Chem.* **390** 19-25
Darken L S 1967 *Trans. Metall. Soc. AIME* **239** 80
de Wijs G 1995 First-principles molecular-dynamics simulations of some ionic liquid alloys *Thesis* Groningen
Geertsma W 1995 in preparation
Geertsma W, Dijkstra J and van der Lugt W 1984 *J. Phys. F: Met. Phys.* **14** 1833
Ichikawa K 1984 *J. Non-Cryst. Solids* **61+62** 35–40
Johnson G K, Geertsma W and Saboungi M-L 1995 to be submitted
Kliche G, Schwartz M and von Schnering H-G 1987 *Angew. Chem. Int. Edn Engl.* **26** 349–51
McGreevy R L 1995 unpublished results
Moffat W G 1984 *The Handbook of Binary Phase Diagrams*
Moore W J 1968 *Physical Chemistry* 4th edn (London: Longmans) p 627
Price D L and Saboungi M-L 1991 *Phys. Rev.* **44** 7289–95
Reijers H T J 1990 Formation of poly-anions in liquid alloys *Thesis* Groningen
Reijers H T J, Saboungi M-L, Price D L and van der Lugt W 1990 *Phys. Rev.* **41** 5661–6
Saar J and Ruppersberg H 1987 *J. Phys. F: Met. Phys.* **17** 305–14
——1988 *Z. Phys. Chem.* **156** 587–91
Saboungi M L 1995 private communication
Saboungi M-L, Geertsma W and Price D L 1990a *Annu. Rev. Phys. Chem.* **41** 207

Saboungi M-L, Johnson G K, Price D L and Reijers R T J 1990b *High Temp. Science* **26** 335–44
Saboungi M-L, Reijers R, Blander M and Johnson G K 1988 *J. Chem. Phys.* **89** 5869–75
Takeda S, Okazaki H and Tamaki S 1985 *Phys. Rev.* B **31** 7452–4
Toukan K, Reijers H J T, Loong C-K, Price D L and Saboungi M-L 1990 *Phys. Rev.* B **41** 11 739–42
Tumidajski P J, Pertric A, Takenaka T, Pelton A D and Saboungi M L 1990 *J. Phys.: Condens. Matter* **2** 209
van der Lugt W 1991 *Phys. Scr.* T **39** 372
van der Lugt W and Geertsma W 1987 *Can J. Phys.* **65** 326
von Schnering H G 1981 *Angew. Chem. Int. Edn Engl.* **20** 33–51
Xu R, de Jonge T and van der Lugt W 1992 *Phys. Rev.* B **45** 12 788–92